AIMS Mathematics, 9(7): 18374–18402.
DOI: 10.3934/math.2024896
Received: 09 February 2024
Revised: 16 May 2024
Accepted: 21 May 2024
Published: 31 May 2024

https://www.aimspress.com/journal/Math

Research article

Fractional heat transfer DPL model incorporating an exponential Rabotnov kernel to study an infinite solid with a spherical cavity

Ahmed E. Abouelregal[1,*], Faisal Alsharif[2], Hashem Althagafi[3] and Yazeed Alhassan[1]

[1] Mathematics Department, College of Science, Jouf University, P.O. Box 2014, Sakaka, Saudi Arabia
[2] Department of Mathematics, College of Science, Taibah University, Al-Madinah Al-Munawarah, Saudi Arabia
[3] Mathematics Department, Faculty of Science, Umm Al-Qura University, Makkah 21955, Saudi Arabia

* **Correspondence:** Email: ahabogal@ju.edu.sa; Tel: +966531095740.

Abstract: The objective of this study was to investigate the thermodynamic reactions of thermoelastic materials by utilizing a modified mathematical fractional thermoelastic model. This model combines a fractional derivative with Rabotnov's exponential kernel and the idea of a two-phase delay, which makes it possible to show thermoelastic behavior more accurately. The model was utilized to investigate an unbounded material with a spherical cavity subjected to a decreasing and shifting heat flux on its inner surface. The problem was solved using analytical approaches, with a strong focus on the Laplace transform. The transform was numerically inverted to provide time-domain results. The study presented graphs that compared the outcomes of utilizing a single kernel fractional derivative with the results obtained using the Rabotnov kernel and fractional order. These graphs showed how the Rabotnov kernel and fractional order affected the physical fields under investigation. This novel theoretical framework has the potential to be advantageous in diverse domains, including engineering, solid mechanics, and materials science.

Keywords: fractional heat conduction; Rabotnov's exponential kernel; phase delays; non-singular kernel; heat flux
Mathematics Subject Classification: 35B35, 37L30, 74F05, 74H10, 80A19

1. Introduction

One of the ongoing investigations that is being conducted on the subject of fractional calculus is the examination of the optimal characterization of fractional operators. Fractional derivatives, which extend differentiation to orders that are not integers, make it possible to do analysis on systems that have fractional dynamics characteristics. The Caputo-Liouville and Riemann-Liouville derivatives are examples of fractional derivatives that are often utilized. These derivatives have been extensively researched and used in a variety of fields [1,2]. However, in recent years, there has been an increase in the number of fractional derivative classifications that have presented alternatives to conventional fractional derivatives [3–6]. The absence of singularities distinguishes these novel derivatives, and their design aims to overcome limitations or deficiencies found in existing derivatives. Researchers have investigated the mathematical features of these unique operators, examining their behavior with various kinds of functions and their interactions with other fractional operators [7]. Scientists have initiated additional research and exploration into the features of these new fractional derivatives, as well as their practical applications, following their introduction. Scientists from a variety of fields, including engineering, signal processing, and physics, are investigating the applicability of these materials [8]. While selecting a particular fractional derivative, one should consider both the nature of the problem at hand and the desired qualities in the solution. It is possible that different variations are better suited for certain applications; the selection process ought to be directed by the requirements and characteristics of the particular problem that is being investigated. Ongoing research attempts to improve the characterization of fractional operators, investigate their mathematical properties, and evaluate the extent to which they can be applied in a variety of domains, taking into account the specific requirements of the problem being addressed [9].

Recent literature has introduced various non-singular fractional derivatives, including the Caputo-Fabrizio, Atangana-Baleanu, and Rabotnov exponential kernel fractional derivatives. These derivatives provide options that are different from ordinary fractional calculus and have unique properties. The Caputo-Fabrizio fractional derivative, first proposed in reference [5], is a non-singular alternative that has found applications in diverse fields. The Atangana-Baleanu fractional derivative also referred to as the Mittag-Leffler kernel fractional derivative, was introduced in [4] and has been applied in practical situations, as demonstrated by references [10–14]. The Rabotnov exponential kernel fractional derivative, which was recently suggested and discussed in [6], is a non-singular fractional derivative that has been successfully applied in real issues, as evidenced by references [15–18]. These examples show how fractional calculus and non-singular fractional derivatives are useful in a wide range of disciplines. Applications encompass a wide range of areas, including physics, engineering, biology, economics, and various others. Also, applications in many fields have proven the effectiveness of these non-singular fractional derivatives in solving many problems.

Thermoelasticity is a field within solid mechanics that studies how materials react to both heat and mechanical stresses. This field focuses on understanding the impact of temperature changes on materials' mechanical properties as well as the generation of thermal stresses due to mechanical deformation [19]. The fundamental equations employed in thermoelasticity theory to characterize material behavior are the equations of motion and the heat conduction equation. The equations of motion, deduced from Newton's second rule of motion, delineate the material's mechanical dynamics

by creating a correlation between stress and strain. These equations incorporate material properties such as elasticity and viscosity and can be solved to ascertain displacement and stress distributions under specified mechanical loads [20]. The heat conduction equation relates the temperature distribution of a material to its heat generating, conduction, and convection properties. It is based on the principles of energy conservation and Fourier's law of heat conduction. The heat conduction equation's solution provides valuable insights into the spatial distribution of temperature within a material due to thermal stresses [21]. Comprehending and forecasting thermal stresses are essential in many engineering applications, such as the development of structures subjected to elevated temperatures, thermal barrier coatings, and thermal management systems. Thermoelasticity theory provides a systematic approach to examining and forecasting the behavior of materials under thermal loading conditions, as well as the resulting thermal stresses [22,23]. It examines the interaction between thermal and mechanical properties.

The Fourier equation for heat conduction states that the rate of heat transfer is directly proportional to the temperature gradient, assuming that heat propagation occurs instantaneously. This implies an almost infinite rate of heat transport. In reality, heat transfer does not occur instantaneously but rather at a finite speed [24]. One can utilize advanced mathematical models, such as hyperbolic heat conduction models or the Cattaneo-Vernotte equation, to precisely mimic heat transfer processes that occur at a finite pace [25–30]. These generalized thermoelasticity models incorporate the time delay associated with heat propagation and offer a more precise depiction of the temperature distribution and heat transmission rates. Generalized thermoelasticity models expand upon traditional thermoelasticity models by incorporating a larger range of physical phenomena and providing a more accurate representation of material behavior under heating conditions.

The incorporation of fractional differentiation into thermoelasticity is a state of the art methodology that has recently garnered significant interest. Fractional calculus offers a mathematical structure for phenomena that involve nonlocality, memory effects, and intricate dynamics. By integrating fractional derivative operators into thermoelastic equations, a new framework is established that allows for differentiation with non-integer orders. This technique is well-suited for representing materials with intricate behaviors, such as viscoelastic materials or those with fractional characteristics, because it accurately accounts for memory effects and interactions across vast distances. By incorporating fractional differentiation, it becomes possible to account for nonlocal and memory-dependent effects in the governing equations. This leads to a more precise representation of the thermal characteristics of materials, particularly those with long-term memory or anomalous diffusion processes.

This paper presents a novel thermoelasticity model that integrates fractional differentiation with two-phase delays by combining a fractional operator with the recently developed Rabotnov exponential kernel. The model is utilized to examine the thermomagnetic characteristics of solid materials, including a spherical hollow subjected to a diminishing and mobile heat flux. The hollow is enclosed and encompassed by a persistent axial magnetic field of uniform thickness. A numerical method was employed to execute Laplace inversions, allowing for the calculation of the temporal

solution. Graphical depictions depict the estimated values for temperature, deformation, thermal stresses, and induced electromagnetic fields. The impact of this new factor on thermoelastic material behavior is evaluated by comparing its results with those obtained via fractional derivatives with a singular kernel. Numerical data is utilized to quantify and assess the reactions of distinct physical domains, taking into account influential factors such as phase delay durations and fractional differential order.

List of symbols

T_0	Environmental temperature	(r, Θ, ϕ)	Cylindrical coordinate
$\gamma = (3\lambda + 2\mu)\alpha_t$	Coupling coefficient	λ, μ	Lame's elastic coefficients
U_i	Displacements	Q	Heat source
S_{ij}	Thermal stresses	$\vec{F}$	Heat flux
α	Fractional order	τ_q	Phase-lag of heat flow
e_{ij}	Strains	τ_θ	Phase-lag of temperature gradient
$\theta = T - T_0$	Temperature change	α	Fractional order
ρ	Density of the material	$\vec{h}$	Induced magnetic field
T	Absolute temperature	$\vec{E}$	Induced electric field
K	Thermal conductivity	$\vec{J}$	Current density
C_e	Specific heat	$\vec{B}$	Magnetic field
α_t	Thermal expansion parameter	μ_0	Magnetic permeability
δ_{ij}	Kronecker delta	R_i	External forces
$\Gamma(\alpha)$	Gamma function		

2. Fractional thermoelastic DPL model derivation

The generalized thermoelasticity governing equations express the relationship between a material's mechanical and thermal properties. The concepts of mass, momentum, and energy conservation derived these equations, which include constitutive relationships connecting displacement, heat, and stress. The theory of generalized thermoelasticity uses the following formulas for isotropic and homogeneous bodies to fully capture these interactions [24–27]:

$$\sigma_{kl} = 2\mu\varepsilon_{kl} + [\lambda\varepsilon_{mm} - \gamma\theta]\delta_{kl}, \tag{2.1}$$

$$2\varepsilon_{kl} = u_{k,l} + u_{l,k}, \tag{2.2}$$

$$\sigma_{kl,l} + R_k = \rho\frac{\partial^2 u_k}{\partial t^2}, \tag{2.3}$$

$$(\lambda + \mu)u_{l,kl} + \mu u_{k,ll} - \gamma\theta_{,k} + R_k = \rho\frac{\partial^2 u_k}{\partial t^2}. \tag{2.4}$$

The following formulation expresses the relationship between energy conservation and heat transport in elastic materials [25]:

$$\rho C_e\frac{\partial\theta}{\partial t} + T_0\gamma\frac{\partial\varepsilon_{kk}}{\partial t} = -\nabla\cdot\vec{F} + Q. \tag{2.5}$$

Advanced and sophisticated models have been created to overcome the constraints of Fourier's law. These encompass altered thermoelastic models, models grounded on fractional calculus, and systems featuring phase delays. Advanced mathematical models are capable of representing heat transport in materials that display nonlocal or memory-based behavior with greater accuracy. The dual-phase-lag (DPL) model [29–31] was developed to include the effects of both limited heat transport and microstructural interactions, which are not accounted for by the conventional Fourier's law. The enhanced version of Fourier's law in the DPL model can be expressed as [30, 31]:

$$\vec{F} + \tau_q\frac{\partial\vec{F}}{\partial t} = -K\left(1 + \tau_\theta\frac{\partial}{\partial t}\right)\nabla\theta. \tag{2.6}$$

The expansion of the traditional heat transfer equation to the fractional heat transmission equation has provided new opportunities for modeling heat transfer in materials with nonlocal or memory-dependent characteristics. These models give a more accurate picture of heat transfer in these materials by including fractional derivatives, which show how heat conduction is affected by what has happened in the past. In the present work, a new formulation of Fourier's law will be presented by replacing the usual time derivative ($\partial/\partial t$) with the fractional time derivative (represented by $D_t^{(\alpha)}$). The introduction of the fractional derivative operator is essential to capture the memory-based behavior of materials subjected to thermal conductivity. In view of this, the modified Fourier fractional law can be represented as follows:

$$\vec{F} + \tau_q^\alpha\ D_t^{(\alpha)}\vec{F} = -K\left(\vec{\nabla}\theta + \tau_\theta^\alpha\ D_t^{(\alpha)}\nabla\theta\right). \tag{2.7}$$

The fractional derivative $D_t^{(\alpha)}$ can be expressed using different fractional derivative operators, including the Caputo [32], Riemann-Liouville, Caputo-Fabrizio (CF) [5], and Atangana-Baleanu (AB) [4] fractional derivatives. Each operator possesses its unique mathematical definition and features, rendering them appropriate for various applications in fractional calculus. In the field of thermoelasticity, the application of the fractional derivative with the Ratbotnov exponential kernel is fascinating. The Ratbotnov exponential kernel, which is explained in reference [6], has unique properties that make it useful for showing certain aspects of thermoelastic behavior. Conventional fractional derivative operators may not adequately address particular memory impacts or nonlocal interactions. The operators for fractional derivatives that are associated with the Caputo [32], CF [5], and AB [4,33] can be represented as:

$${}^{C}D_t^{(\alpha)}\hbar(x,t) = \frac{1}{\Gamma(1-\alpha)}\int_0^t (t-\xi)^{-\alpha}\frac{\partial\hbar(x,\xi)}{\partial\xi}d\xi, \alpha \in (0,1], \tag{2.8}$$

$$ {}^{CF}_{\ }D_t^{(\alpha)}\hbar(x,t) = \frac{1}{1-\alpha}\int_0^t \dot{\hbar}(x,\xi)\mathrm{Exp}\left(-\frac{\alpha}{(1-\alpha)}(t-\xi)\right)d\xi, \tag{2.9} $$

$$ {}^{AB}_{\ }D_t^{(\alpha)}\hbar(x,t) = \frac{1}{1-\alpha}\int_0^t \dot{\hbar}(x,\xi)E_\alpha\left(-\frac{\alpha}{(1-\alpha)}(t-\xi)^\alpha\right)d\xi, \tag{2.10} $$

where $E_\alpha(z)$ denotes the enhanced Mittag-Leffler function.

One possible representation of the Rabotnov exponential function (REF) of order $\alpha \in \mathbb{R}^+$ with parameter $\xi \in \mathbb{R}^+$ is the series that is illustrated below [34,35]:

$$ \mathcal{R}_\alpha(\chi z^\alpha) = \sum_{k=0}^{\infty}\frac{\chi^k z^{(k+1)(\alpha+1)-1}}{\Gamma[(1+\alpha)(k+1)]},\ z \in \mathbb{C}. \tag{2.11} $$

Using the non-singular kernel of the Rabotnov fractional-exponential function, the following is the definition of the generic fractional-order derivative of the Liouville-Caputo type [6,36]:

$$ {}^{RE}_{a}D_t^{\alpha}\hbar(x,t) = \int_a^t \dot{\hbar}(x,\xi)\mathcal{R}_\alpha(-\chi(t-\xi)^\alpha)\,d\xi. \tag{2.12} $$

The fractional Yang-Abdel-Aty-Cattani (YAC) derivative given by the Laplace transform takes the following form [4]:

$$ \mathcal{L}[{}^{RE}_{a}D_t^{\alpha}\hbar(x,t)] = \frac{1}{s^{\alpha+1}}\frac{1}{1+\chi s^{-(\alpha+1)}}[s\mathcal{L}[\hbar(x,t)] - \hbar(x,0)]. \tag{2.13} $$

Rabotnov's fractional order operator application provides a robust method for understanding and examining the mechanics of structures with hereditary flexibility. Various fields have shown the advantages of this technology's implementation, enabling the simulation and prediction of material behavior in a wide range of situations.

The following formula, which combines Eqs (2.5) and (2.7), may be used to obtain the modified version of the generalized DPL heat conduction theory with phase delays that contain fractional operators:

$$ \left(1 + \tau_q^\alpha\, D_t^{(\alpha)}\right)\left[\rho C_E\frac{\partial\theta}{\partial t} + T_0\gamma\frac{\partial\varepsilon_{kk}}{\partial t} - Q\right] = \left(1 + \tau_\theta^\alpha\, D_t^{(\alpha)}\right)\left(\nabla.(K\,\nabla\theta)\right). \tag{2.14} $$

The combination of Maxwell's equations and the Lorentz force law provides a comprehensive mathematical foundation for understanding electromagnetic phenomena. These equations describe the characteristics of electromagnetic fields, the movement of electromagnetic waves, and the interaction between electromagnetic fields, charges, and currents. Experimental testing has extensively validated Maxwell's equations, confirming their accuracy and reliability. As a result, these equations have been crucial to the progress of technology in several domains, such as power production, transmission systems, telecommunications, optics, and others. Their fundamental importance in these fields underscores their tremendous influence on contemporary technology and scientific understanding. The equations formulated by Maxwell to represent the electromagnetic control system can be written

as [37,38]:

$$\nabla \times \vec{h} = \vec{J}, \quad -\mu_0 \frac{\partial}{\partial t}(\vec{h}) = \nabla \times \vec{E}, \quad \vec{E} = -\mu_0 \left(\frac{\partial \vec{u}}{\partial t} \times \vec{B}\right), \\ \vec{h} = \nabla \times \left(\vec{u} \times \vec{B}\right), \ \nabla \cdot \vec{h} = 0. \tag{2.15}$$

The following relationship can also be used to determine the Maxwell stress, M_{ij}, [39,40]

$$M_{ij} = \mu_0 \left[B_i h_j + B_j h_i - B_k h_k \delta_{ij}\right]. \tag{2.16}$$

The Lorentz force is a fundamental principle in classical electromagnetism that is essential for comprehending and forecasting the actions of charged particles in electromagnetic fields. It is widely regarded as one of the most pivotal notions in the field of physics. The Lorentz force has a wide range of applications, such as in electric motors, particle accelerators, and the movement of charged particles in electromagnetic waves. The Lorentz force can be determined by utilizing the relationship:

$$\vec{L} = \mu_0 \left(\vec{J} \times \vec{B}\right). \tag{2.17}$$

3. Applicable problem formulation

This section will analyze the behavior of an infinite thermoelastic material with a spherical cavity when subjected to various heat fluxes. According to Figure 1, the thermoelastic material is assumed to occupy the area where $R \leq r \leq \infty$ and includes a spherical hollow with a radius R. This analysis directly applies to the suggested model. In order to analyze and address the issue, we will employ the spherical polar coordinate system (r, Θ, ϕ), with the coordinate origin situated in the middle of the cavity. At first $T = T_0$, the material is presumed to be unreactive, uniform, have the same properties in all directions, and be capable of conducting electricity. Furthermore, it is believed that the spherical cavity is constrained. Additionally, it is presumed that the cavity is submerged in a constant and axial external magnetic field represented by $\vec{B} = (0,0,H_0)$. Given the symmetry of the issue, we will assume that the field variables are only dependent on the radial distance r and the instantaneous time t. Additionally, it is presumed that the field variables possess finite values and exhibit behavior that aligns with their physical characteristics as the radial distance r approaches infinity (∞). This issue type finds several applications in fields such as engineering, geophysics, astronomy, airplanes, missiles, nuclear reactors, and power plants. These applications include intricate geometries and boundary conditions.

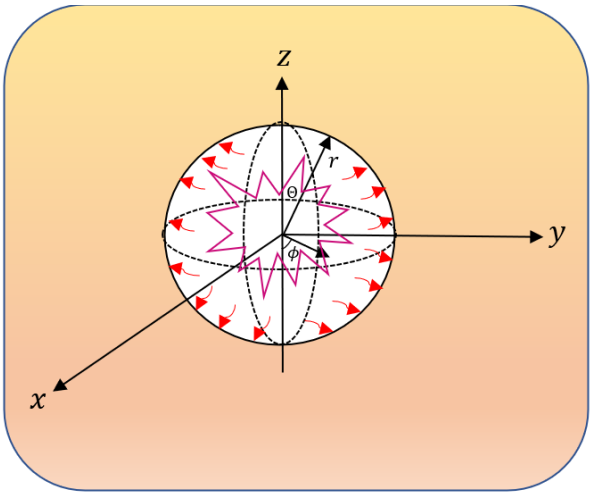

Figure 1. Configurational representation of an infinite elastic medium with a spherical hole.

Due to the fact that the issue is one-dimensional, the displacement vector and temperature θ may be characterized as a function of the radial distance r and the instantaneous time t. As a result, the governing formulas can be represented as follows:

$$u_r = u(r,t),\ u_\Theta(r,t) = u_\phi(r,t) = 0, \tag{3.1}$$

$$e_{rr} = \frac{\partial u}{\partial r},\ e_{\Theta\Theta} = e_{\phi\phi} = \frac{u}{r}, \tag{3.2}$$

$$e = \nabla \cdot u = \frac{\partial u}{\partial r} + \frac{2u}{r} = \frac{1}{r^2}\frac{\partial (r^2 u)}{\partial r}, \tag{3.3}$$

$$S_{rr} = \frac{\lambda}{r^2}\frac{\partial (r^2 u)}{\partial r} + 2\mu\frac{\partial u}{\partial r} - \gamma\theta, \tag{3.4}$$

$$S_{\Theta\Theta} = \frac{\lambda}{r^2}\frac{\partial (r^2 u)}{\partial r} + 2\mu\frac{u}{r} - \gamma\theta, \tag{3.5}$$

$$\frac{\partial S_{rr}}{\partial r} + \frac{2}{r}S_{rr} - \frac{2}{r}S_{\Theta\Theta} + L_r = \rho\frac{\partial^2 u}{\partial t^2}. \tag{3.6}$$

When a fixed magnetic field vector $\vec{B} = (0,0,H_0)$ is present, the motion of the material points in the medium produces an induced magnetic field $\vec{h}$ in the ϕ-axis direction. In terms of the fixed magnetic field $\vec{B}$ and the displacement vector $\vec{u}$, the induced magnetic field $\vec{h}$ may be written as follows:

$$\vec{h} = -H_0\left(0,0,\frac{1}{r^2}\frac{\partial (r^2 u)}{\partial r}\right). \tag{3.7}$$

Next, along the direction of the Θ-axis, the induced magnetic field $\vec{h}$ produces an induced electric field $\vec{E}$, which may be written as follows:

$$\vec{E} = \mu_0 H_0^2 \left(0, \frac{\partial u}{\partial t}, 0\right). \tag{3.8}$$

Additionally, the induced magnetic field $\vec{h}$ may be used to represent the electric current density $\vec{J}$ as follows:

$$\vec{J} = -H_0 \left(0, \frac{\partial}{\partial r}\left(\frac{1}{r^2}\frac{\partial (r^2 u)}{\partial r}\right), 0\right). \tag{3.9}$$

When substituting Eqs (3.8) and (3.9) into Eqs (2.16) and (2.17), the radial Lorentz force L_r and the Maxwell stress components M_{rr} can be expressed as follows:

$$L_r = \mu_0 \left(\vec{J} \times \vec{B}\right)_r = \mu_0 H_0^2 \frac{\partial}{\partial r}\left(\frac{1}{r^2}\frac{\partial (r^2 u)}{\partial r}\right), \quad M_{rr} = \mu_0 H_0^2 \frac{1}{r^2}\frac{\partial (r^2 u)}{\partial r}. \tag{3.10}$$

The modified formulation of the extended DPL heat transfer theory with phase delays that includes fractional operators can be expressed as follows:

$$\left(1 + \tau_\theta^\alpha \, D_t^{(\alpha)}\right)\nabla^2 \theta = \left(1 + \tau_q^\alpha \, D_t^{(\alpha)}\right)\left[\frac{1}{k}\frac{\partial \theta}{\partial t} + \frac{\gamma T_0}{K}\frac{\partial e}{\partial t}\right], \qquad \frac{K}{\rho C_e} = k. \tag{3.11}$$

Following the utilization of Eqs (3.4) and (3.5), the equation of motion (3.6) may be constructed as follows:

$$\left(\frac{\lambda + 2\mu}{\rho} + \frac{\mu_0 H_0^2}{\rho}\right)\frac{\partial e}{\partial r} = \frac{\gamma}{\rho}\frac{\partial \theta}{\partial r} + \frac{\partial^2 u}{\partial t^2}. \tag{3.12}$$

After applying the factor $\partial/\partial r + 2/r$ to both sides of the Eq (3.12), one concludes that the following equation is obtained:

$$\rho(c_0^2 + a_0^2)\nabla^2 e = \gamma \nabla^2 \theta + \rho \frac{\partial^2 e}{\partial t^2}, \tag{3.13}$$

where $\nabla^2 = \frac{1}{r^2}\frac{\partial}{\partial r}\left(r^2 \frac{\partial}{\partial r}\right)$, $c_0^2 = \frac{\lambda + 2\mu}{\rho}$ and $a_0^2 = \frac{\mu_0 H_0^2}{\rho}$.

Dimensionless quantities are commonly employed to simplify and standardize the governing equations. Below are frequently used formulas for nondimensional variables.

$$\begin{gathered}\{r', u'\} = \frac{c_0}{k}\{r, u\}, \ \ \{t', \tau_\theta', \tau_q'\} = \frac{c_0^2}{k}\{t, \tau_\theta, \tau_q\}, \ \ \theta' = \frac{\gamma}{\rho c_0^2}\theta, \\ \{S_{ij}', M_{ij}'\} = \frac{1}{\rho c_0^2}\{S_{ij,} M_{rr}\}.\end{gathered} \tag{3.14}$$

Neglecting the prime, we can express the formulas for the fundamental equations in nondimensional form as follows:

$$\left(1 + \tau_\theta^\alpha D_t^{(\alpha)}\right)\nabla^2 \theta - \frac{\partial}{\partial t}\left(1 + \tau_q^\alpha D_t^{(\alpha)}\right)\theta = \varepsilon \frac{\partial}{\partial t}\left(1 + \tau_q^\alpha D_t^{(\alpha)}\right)e, \tag{3.15}$$

$$a_1\nabla^2\theta = \left(\nabla^2 - a_2\frac{\partial^2}{\partial t^2}\right)e, \tag{3.16}$$

$$S_{rr} = \frac{1}{r^2}\frac{\partial(r^2u)}{\partial r} + \frac{4\beta^2}{r}u - \theta, \tag{3.17}$$

$$S_{\Theta\Theta} = (1-2\beta^2)\frac{1}{r^2}\frac{\partial(r^2u)}{\partial r} - \frac{2\beta^2}{r}u - \theta, \tag{3.18}$$

where

$$\begin{gathered}\beta^2 = \mu/(\lambda+2\mu),\ \varepsilon = T_0\gamma^2/(\rho^2c_0^2C_e), a_1 = g/(c_0^2+a_0^2),\\ a_2 = \rho c_0^2/(c_0^2+a_0^2),\quad g = \gamma T_0/\rho.\end{gathered} \tag{3.19}$$

At the outset of the analysis, we will impose initial circumstances that are representative of the state of matter before applying any external perturbations. These conditions will include the following:

$$u(r,0) = 0 = \frac{\partial u(r,0)}{\partial t}, S_{rr}(r,0) = 0 = S_{\Theta\Theta}(r,0), \theta(r,0) = 0 = \frac{\partial\theta(r,0)}{\partial t}. \tag{3.20}$$

These starting conditions, the boundary conditions established by the material's composition and unique qualities, and the external perturbations applied to it can all be used to solve the governing equations. In this instance, it is expected that the heat flow F diminishes exponentially with instantaneous time t and travels at a constant velocity ϑ in the direction of the cavity axis. The following relationship characterizes this behavior [41]:

$$F = F_0\, e^{-\omega t}\,\delta(r-\upsilon t),\ ,\ t>0,\ \text{at}\quad r=a. \tag{3.21}$$

The variables in the equation are defined as follows: F_0 represents the starting heat flow, ω represents the exponential decay parameter, and $\delta(r-\upsilon t)$ represents the Dirac delta function, which indicates that the heat flow is concentrated at the position $r=\upsilon t$. Taking into account the dimensionless quantities (31) and substituting from (38) into the modified Fourier law (7), we obtain the following boundary condition:

$$\left(1+\tau_\theta D_t^{(\alpha)}\right)\frac{\partial\theta(r,t)}{\partial r} = -F_1\left(1+\tau_q D_t^{(\alpha)}\right)e^{-\omega t}\,\delta(r-\upsilon t),\ \ F_1 = \frac{F_0\rho k c_0}{\gamma}. \tag{3.22}$$

It was considered that the material cannot move or deform on its surface, meaning that the surface displacement $u(r,t)$ is restricted. Therefore, the spherical gap surface is subject to the following mechanical constraint:

$$u(r,t) = 0\ \ \text{at}\ r=a. \tag{3.23}$$

4. Solution of the problem

In the study of thermoelastic materials, the Laplace transform is often used to move the governing equations from the space-time domain to the space domain, where they are easier to solve. The following is the definition of the Laplace transform of any function $g(r,t)$:

$$\bar{g}(r,s) = \int_0^{\infty} g(r,t)e^{-st}dt, \tag{4.1}$$

where s is a complex number with a positive real part ($Re(s) > 0$) and $\bar{g}(r,s)$ denotes the transformed function. We use the inverse Laplace transform to restore the changed fields to their original state in the time domain. This transform is defined as follows:

$$g(r,s) = \frac{1}{2\pi i}\int_{\Upsilon-\infty}^{\Upsilon+\infty} \bar{g}(r,t)e^{st}ds, \tag{4.2}$$

where Υ is a real number greater than the real part of all the singularities of $\bar{g}(r,s)$.

Using the Laplace transform on the fundamental equations, we are able to obtain the following:

$$(\nabla^2 - \alpha_1)\bar{\theta} = \alpha_2\nabla^2\bar{e}, \tag{4.3}$$

$$a_1\bar{\theta} = (\nabla^2 - a_2 s^2)\bar{e}, \tag{4.4}$$

$$\bar{S}_{rr} = 4\beta^2\frac{\overline{u}}{r} + \bar{e} - \bar{\theta}, \tag{4.5}$$

$$\bar{S}_{\Theta\Theta} = -2\beta^2\frac{\overline{u}}{r} + (1-2\beta^2)\bar{e} - \bar{\theta}, \tag{4.6}$$

where

$$\alpha_1 = \frac{s\left(1+\alpha_0\tau_q^{\alpha}\right)}{\left(1+\alpha_0\tau_{q\theta}^{\alpha}\right)}, \alpha_2 = \frac{s\varepsilon\left(1+\alpha_0\tau_q^{\alpha}\right)}{\left(1+\alpha_0\tau_{q\theta}^{\alpha}\right)},\ \alpha_0 = \frac{s}{s^{\alpha+1}}\frac{1}{1+\chi s^{-(\alpha+1)}}. \tag{4.7}$$

Through the elimination method we can separate Eqs (4.3) and (4.4) and obtain the following independent equations:

$$\begin{aligned} \nabla^4\bar{e} - \delta_1\nabla^2\bar{e} + \delta_2\bar{e} = 0, \\ \nabla^4\bar{\theta} - \delta_1\nabla^2\bar{\theta} + \delta_2\bar{\theta} = 0, \end{aligned} \tag{4.8}$$

where

$$\delta_1 = \alpha_1 + s^2 a_2 + \alpha_2 a_1, \quad \delta_2 = \alpha_1 s^2 a_2. \tag{4.9}$$

Within Laplace transforms, the temperature and displacement can be obtained by solving these separate equations independently as follows:

$$\bar{e}(r,s) = \frac{\alpha_2}{\sqrt{r}}\left[A_1\mu_1^2 K_{1/2}(\mu_1 r) + A_2\mu_2^2 K_{1/2}(\mu_2 r)\right], \tag{4.10}$$

$$\bar{\theta}(r,s) = \frac{1}{\sqrt{r}}\left[(\mu_1^2 - \alpha_1)A_1 K_{1/2}(\mu_1 r) + (\mu_2^2 - \alpha_1)A_2 K_{1/2}(\mu_2 r)\right]. \tag{4.11}$$

The boundary conditions give the integrative coefficients A_i, where $i = 1$, 2, and 3 are the respective parameters. Also, $K_{1/2}(\mu_1 r)$ represents the second category of modified Bessel functions with an order of 1/2. Furthermore, the coefficients μ_1^2 and μ_2^2 are the characteristic roots of differential equations. The roots of this equation can be expressed as follows:

$$\mu_1^2 = \frac{\delta_1 + \sqrt{\delta_1^2 - 4\delta_2}}{2}, \quad \mu_2^2 = \frac{\delta_1 - \sqrt{\delta_1^2 - 4\delta_2}}{2}. \tag{4.12}$$

It is possible to arrive at a solution for the dimensionless displacement function $\bar{u}(r,s)$ by taking into account the relationship between the Laplace transforms of the displacement component, $\bar{u}(r,s)$, and the function $\bar{e}(r,s)$ as follows:

$$\bar{u}(r,s) = -\frac{\alpha_2}{\sqrt{r}}\left[A_1\mu_1 K_{3/2}(\mu_1 r) + A_2\mu_2 K_{3/2}(\mu_2 r)\right]. \tag{4.13}$$

By substituting the previous solutions into Eqs (4.5) and (4.6), we can derive the following solutions for dimensionless thermal stresses:

$$\begin{aligned}\bar{S}_{rr}(r,s) = {} & \frac{1}{\sqrt{r}}\left[(\alpha_2\mu_1^2 - \mu_1^2 + \alpha_1)K_{1/2}(\mu_1 r) - \frac{4\beta^2\mu_1\alpha_2}{r}K_{3/2}(\mu_1 r)\right]A_1 \\ & + \frac{1}{\sqrt{r}}\left[(\alpha_2\mu_2^2 - \mu_2^2 + \alpha_1)K_{1/2}(\mu_2 r) - \frac{4\beta^2\mu_2\alpha_2}{r}K_{3/2}(\mu_2 r)\right]A_2,\end{aligned} \tag{4.14}$$

$$\begin{aligned}\bar{S}_{\Theta\Theta}(r,s) = {} & \left[(\alpha_2\mu_1^2(1-2\beta^2) - \mu_1^2 + \alpha_1)K_{1/2}(\mu_1 r) + \frac{2\beta^2\mu_1\alpha_2}{r}K_{3/2}(\mu_1 r)\right]A_1 \\ & + \left[(\alpha_2\mu_2^2(1-2\beta^2) - \mu_2^2 + \alpha_1)K_{1/2}(\mu_2 r) + \frac{2\beta^2\mu_2\alpha_2}{r}K_{3/2}(\mu_2 r)\right]A_2.\end{aligned} \tag{4.15}$$

By inserting the solutions of the displacement component $\bar{u}(r,s)$ into expression (3.10) we can derive the solution to the Maxwell stress $\bar{M}_{rr}$ in the Laplace transform field

$$\bar{M}_{rr}(r,s) = \frac{a_0^2\alpha_2}{c_0^2\sqrt{r}}\left[A_1\mu_1^2 K_{1/2}(\mu_1 r) + A_2\mu_2^2 K_{1/2}(\mu_2 r)\right]. \tag{4.16}$$

In the field of Laplace transform, conditions (3.22) and (3.23) can be expressed as follows:

$$\frac{\partial\bar{\theta}(r,s)}{\partial r} = -\frac{\alpha_0 F_1}{\upsilon}e^{-\Omega r}, \quad \Omega = \frac{\omega+s}{\upsilon}, \quad r = a, \tag{4.17}$$

$$\bar{u}(r,s) = 0, \qquad r = a. \tag{4.18}$$

We can obtain the parameters $A_i, \ = 1, 2$ by substituting Eqs (4.11) and (4.13) into the boundary conditions (4.17) and (4.18), and then solving the two equations.

5. Laplace inversions

The present investigation presents a resilient numerical technique for Laplace inversion in diverse domains, with a focus on dependability, practicality, and accuracy. This innovative approach uses a methodology based on the extension of Fourier series to estimate inverse Laplace transforms. This technique easily calculates inverse Laplace transforms by describing functions as combinations of Fourier series components, making it widely applicable in engineering and scientific fields [42]. This

approach offers several key advantages, such as its high level of precision, flexibility to adapt to different situations, and capacity to handle a wide range of jobs, including some that are difficult to compute using other methods. The approach's accuracy depends on the careful selection of Fourier series terms [43]. Validation and verification are critical for ensuring that the approach is accurate and reliable. This involves adhering to beginning and boundary conditions, as well as governing equations.

When converting any field $\bar{H}(r,s)$ in a Laplace space field into a space-time field $H(r,t)$, the numerical method based on the following Fourier series extension will be used [44]:

$$H(r,t)=\frac{e^{\xi t}}{\tau_1}\left(\frac{\bar{H}(\xi)}{2}+Re\sum_{k=1}^{N_0}e^{ik\pi t/\tau_1}\bar{H}(\xi+ik\pi/\tau_1)\right),\quad 0\le t\le 2\tau_1. \tag{5.1}$$

In order to implement this approach, a computer program was created using the high-level programming language mathematica, which was specifically designed for numerical computing purposes.

6. Special cases

This section presents a collection of unique theories of thermoelasticity. These theories may be obtained as particular instances of the existing model, either with or without the inclusion of fractional derivative operators or delay phase periods. This indicates that the existing model is a versatile and potent tool for explaining the behavior of thermoelastic materials across a broad spectrum of circumstances.

6.1. Thermoelastic models

By disregarding fractional differentiation and setting the fractional order $\alpha=1$, we can generate several forms of thermoelastic models. This is done in the fundamental equations, and only the parameters τ_θ and τ_q are taken into consideration. The different types of thermoelastic models can be obtained by considering different values of the phase lags τ_θ and τ_q, as follows:

Coupled thermoelastic model (CTE): This model is achieved when both τ_θ and τ_q are equal to zero. In this scenario, there is no time delay between the heat flux ($\vec{F}$) and temperature gradient ($\nabla\theta$).

Single-phase-lag thermoelastic (SPL-TE) model: This model may be achieved when τ_θ is equal to zero and τ_q is greater than zero. In this scenario, there is no delay in the timing of $\nabla\theta$, but there is a delay in the timing of $\vec{F}$ and the mechanical reaction. The alternative name for this concept is the Lord-Shulman theory of thermoelasticity.

DPL thermoelastic (DPL-TE) model: This model is achieved when both τ_θ and τ_q are greater than zero. In this scenario, there is a delay in time between $\vec{F}$ and $\nabla\theta$. This model incorporates the limited speed at which heat spreads.

6.2. Fractional models of thermoelasticity

By using the fractional differential operators $D_t^{(\alpha)}$, where $\alpha\in(0,1)$, one can derive the two fractional thermoelasticity models as follows:

SPL fractional thermoelastic (SPL-FTE) model: This model can be obtained if $\tau_\theta = 0$ and $\tau_q > 0$. In this case, the fractional differential operator $D_t^{(\alpha)}$ is applied only to the $\vec{F}$ term, while $\nabla\theta$ is still described by the classical time derivative. This model considers memory and the historical impacts of the substance.

DPL fractional thermoelastic (DPL-FTE) model: This model is achieved when both τ_θ and τ_q are greater than zero. In this particular instance, the fractional differential operator is applied to both the heat flux and $\nabla\theta$ components. This is done to represent the reality that the memory and historical impacts of the material have an impact on both $\vec{F}$and $\nabla\theta$.

7. Numerical results and discussions

The previous sections have presented an innovative theoretical model for thermoelasticity, which includes the integration of several fractional operators. We used this framework to analyze the behavior of a thermoplastic solid with unlimited elasticity. The solid has a spherical cavity and is exposed to a magnetic field of constant intensity. This section will contain numerical analysis and findings about the material's displacement, temperature, and thermomechanical stress fields. We will consider the mechanical properties of copper in our numerical calculations and analysis. We aim to utilize these calculations to comprehend the impact of a spherical cavity and a constant-intensity magnetic field on the thermoelastic properties of copper. Our goal is to understand how the material reacts to these conditions by looking at how the displacement, temperature, and thermomechanical stress fields are arranged in space and to find any interesting patterns or phenomena. The following are the physical characteristics of the Cu material at $T_0 = 298$ K [45,46]:

$$\rho = 8954\ \text{kg/m}^3\,, \{\lambda, \mu\} = \{7.76, 3.86\} \times 10^{10}\text{kg/ms}^2\,, H_0 = 10^7\text{Am}^{-1}$$
$$K = 386\ \text{W/mK}\,, \quad C_E = 383.1\ \text{J kg/K}\,, \quad \alpha_t = 5 \times 10^{-7}\ 1/\text{K},$$
$$t = 0.12\text{s}, \qquad \mu_0 = 12.6 \times 10^{-7}\ \text{Hm}^{-1}, \quad F_0 = 1, \omega = 0.1\,.$$

The outcomes derived from the computational examination of physical phenomena will be showcased and assessed using graphical representations. The goal of these graphs is to validate the suggested model and enable a comparison between various fractional differentiation operators.

7.1. Comparison of fractional derivative operators

Various values of the fractional-order coefficient are considered in order to carry out the numerical computations. The suggested model is used to analyze the physical behavior of different physical fields. The figures show the difference in results between the nonlocal fractional operator (the new YAC) [6] and the standard Riemann-Liouville fractional model (RL). They also show what happens when there is no fractional differentiation ($\alpha = 1$). The goal of comparing fractional parameters and conventional derivatives is to ascertain the relative efficacy of these operators in mitigating heat waves from a physical standpoint. We base the comparisons on the attributes of the operators, such as their precision, steadfastness, and efficacy.

Figures 2–6 illustrate the changes in the distribution of radial displacement u, temperature change

θ, and stress components S_{rr} and $S_{\Theta\Theta}$ as the radial coordinate r varies. The forms are displayed with fixed values of υ $\upsilon = 5$, $\omega = 15$, $\tau_q = 0.2$, and $\tau_\theta = 0.1$, and with a single value of the fractional order, $\alpha = 0.8$. The study compared the outcomes of nonlocal fractional operators and non-singular kernels, specifically the CF, AB, and YAC fractional models, with the traditional RL fractional model. Additionally, the scenario where fractional differentiation is absent ($\alpha = 1$) was also examined.

Fractional differential factors, which take different forms, have a significant impact on the studied thermophysical fields. The findings also revealed that the fractional order values and the specific type of fractional differential operator influence how thermal and mechanical waves reach their stable states. The literature has cited these results, including those listed in reference [47]. Furthermore, it was discovered that raising the value of the fractional parameter results in an increase in the transmission speed of the analyzed waves near the cavity surface. This is due to the fact that heat flow already exists at the beginning of the waves that are passing through the body, but it diminishes at a quicker rate as the waves penetrate deeper into the medium [48]. Because fractional operators are nonlocal, they depend on the values of the function at all locations in the interval $[0, t]$, rather than simply at the point t. This causes the heat flow to drop more quickly than it would otherwise.

Figures 2 through 6 demonstrate that only within a specific region can we obtain the nonzero values of dynamical temperature, radial displacement, and pressure after determining the instant in time. All the numerical values represent zero outside that zone. As a result, this provides an explanation for why generalized models of thermoelasticity predict that the rate of heat transmission in a thermal medium is restricted. The standard theories of heat transfer, on the other hand, predict that the velocity of thermal and mechanical waves is unbounded which is practically reported by [49]. The comparison results indicate that fractional coefficients are more efficient at mitigating heat waves than standard derivatives. The presence of fractional coefficients results in a dampening effect on the heat waves, leading to a decrease in both their amplitude and frequency [50]. The nonlocal characteristic of the fractional parameters, determined by the function values over the whole interval $[0, t]$, rather than just at the point t, causes the damping effect. Conversely, the usual derivatives are localized and rely on the function's values at a specific point t rather than considering all points throughout the interval $[0, t]$. The localized character of conventional derivatives renders them less useful in mitigating heat waves, as they lack the dampening effect seen by fractional indices.

Figure 2 displays the variations in temperature patterns based on the distance variable for several fractional differential operators and two distinct values of the fractional order factor α. Figure 2 demonstrates that the fractional order coefficient exerts a substantial impact on the dynamics of temperature variation inside the elastic medium. One may also note that the temperature θ attains its maximum value near the surface of the spherical cavity as a result of the existence of a flowing heat flux and thereafter diminishes progressively as it advances away from the cavity until it approaches zero. These observations support the idea that a heat wave can only travel at limited speeds within elastic media.

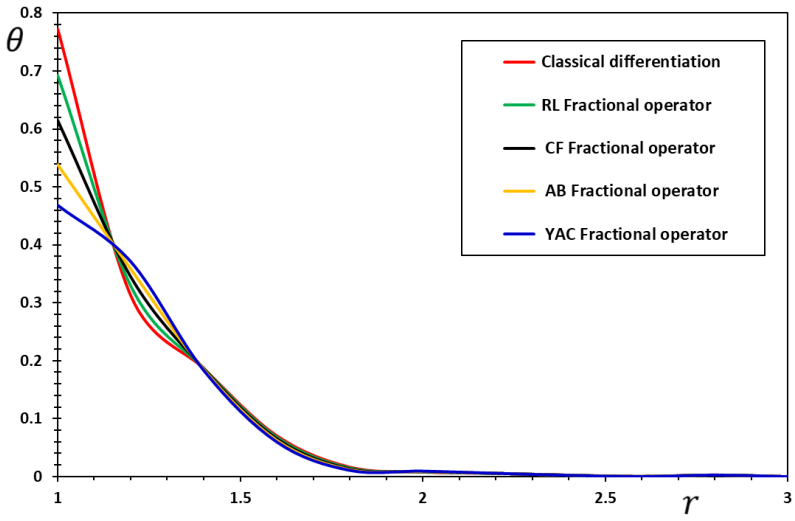

Figure 2. Variation in the temperature θ for various fractional operator.

An important observation that must be taken into account is that the results of the thermoelastic model without the fractional actuator ($\alpha = 1$) give higher temperature values than in the case of the presence of the fractional differential actuator (RL, CF, AB, and YAC) as concluded in [51,52]. Furthermore, based on the data presented, it is evident that the conventional fractional derivative and the fractional derivatives associated with Caputo produce significantly larger physical fields in the vicinity of the disturbance region than CF, AB, the exponential Ratputnov kernel (YAC), and the latter, which yields the smallest values (see [18]).

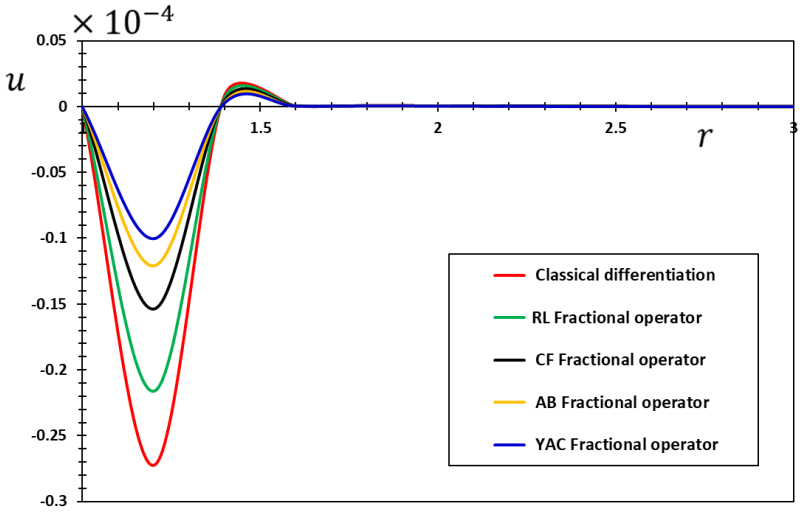

Figure 3. Variation in the displacement u for various fractional operator.

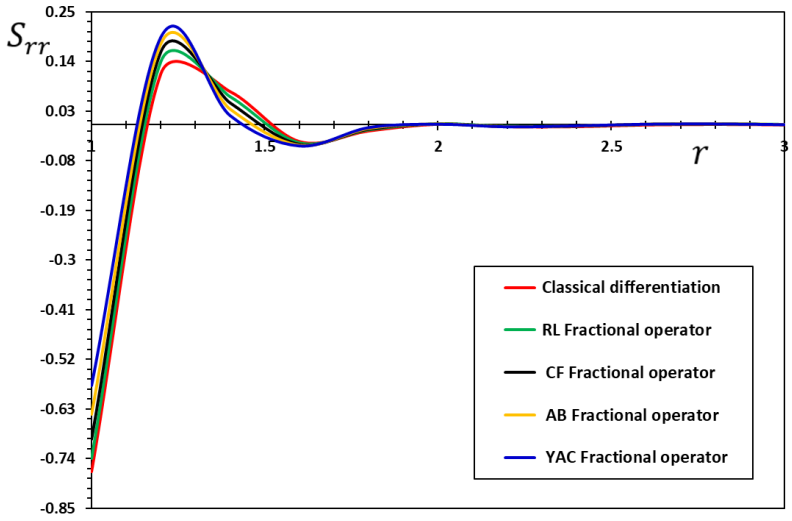

Figure 4. Variation in the radial stress S_{rr} for various fractional operator.

Figure 3 illustrates the variation in the displacement field u as a function of the distance r and the differential actuator. The presence of the fractional parameter α has a dramatic impact on the curves of the displacement field. The displacement values u show an upward trend as the distance increases, reaching their maximum points, then falling and gradually disappearing until they get closer to zero. It was discovered that all displacement curves seem to have zero values from the surface of the gap because the surface is constrained. This was done in order to comply with the criteria of mechanical constraints that were placed on the problem itself. The validity of the method that was applied and the validity of the numerical results obtained as a result are verified. Figure 3 demonstrates that the presence of the fractional differentiation operator leads to varying amounts of displacement u in different locations of the medium. As demonstrated in [18], the displacement in the YAC fractional differential actuator is much smaller than that of other fractional actuators.

The impact of fractional operators (RL, CF, AB, and YAC) on the behavior of the radial stress S_{rr} and hoop pressure $S_{\Theta\Theta}$ distributions with varying radial coordinates r is depicted in Figures 4 and 5. According to the figures, the stresses (S_{rr} and $S_{\Theta\Theta}$) begin with negative values and progressively grow until they reach their maximum value at a distance from the intermediate gap's surface. After that, as the distance increases, the pressures progressively drop until they vanish outside of the turbulence zone. The findings indicate that the addition of fractional operators to the thermoelasticity model significantly affects the distributions of thermal stresses [53]. The curves show that the nonlocal fractional operators (CF, AB, and YAC) lead to smaller amounts of thermal stress than when the fractional differentiation disappears ($\alpha = 1$) and when the standard fractional model is used (RL).

The numerical results depicted in Figures 4 and 5 offer valuable insights into the impact of various fractal factors on thermal stresses. The findings indicate that the magnitudes of these thermal stresses might vary, either increasing or decreasing, depending on the specific fractional derivative factor employed. The contrast highlights the impact of the choice of the fractional operator on the sensitivity of thermal stress responses. The graphs show that these stresses increase dramatically near the

cylindrical cavity, before gradually decreasing within the infinite medium and eventually disappearing. It is crucial to emphasize that in the turbulent zone around the cavitation, the stresses primarily exhibit compressive behavior. This discovery aligns with the theoretical knowledge that compressive stresses are a characteristic of cavitation occurrences in turbulent flows. It is very important to use a fractional differential actuator instead of a regular differential actuator when changing how mechanical waves travel in the heat conduction equation. More precisely, it hinders the rapid propagation of these waves in the medium, resulting in a more accurate progression of the thermal and mechanical fields over time which is practically reported by [53]. As a result, this study highlights the importance of choosing the appropriate fractional operator to effectively capture the complex interaction between thermal and mechanical fields in such situations.

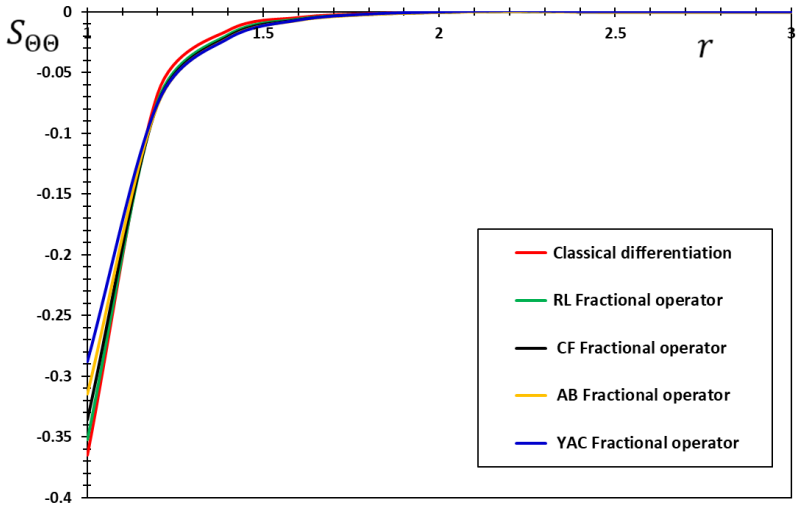

Figure 5. Variation in the hoop stress $S_{\Theta\Theta}$ for various fractional operator.

Figure 6 illustrates the impact of fractional differentiation variables on the distribution of Maxwell stress M_{rr}. The shape curves demonstrate a quick decrease in the Maxwell stress as the distance from the cavity rises. This discovery suggests that the impact of the magnetic field is instantaneous and confined to a specific region. The results indicate that the inclusion or exclusion of fractional components has a little impact on the numerical values of the Maxwell stress, resulting in modest drops or increases. This shows that changes in the fractional parameter have a negligible impact on the Maxwell stress (M_{rr}) characteristics and dynamics.

Traditional fractional derivatives have been thoroughly examined and utilized in several domains, however they may not consistently encompass the nonlocal impacts observed in intricate systems. Although the Caputo-related derivatives, CF, AB, and exponential Ratputnov kernel fractional derivatives (YAC) have common characteristics in terms of being nonlocal and capable of representing intricate systems, they vary in terms of their unique kernels and mathematical qualities. The selection of a suitable fractional derivative operator depends on the specific problem and the intended properties of the solution [54].

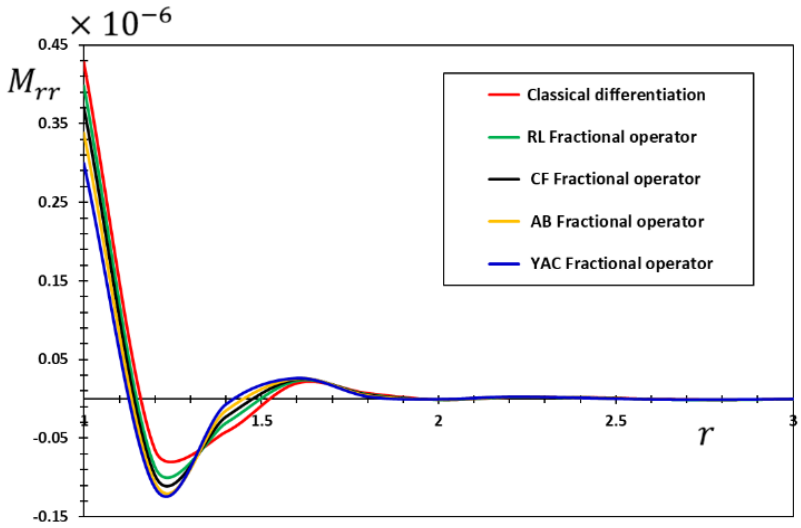

Figure 6. Variation in the Maxwell's stress M_{rr} for various fractional operator.

The comparisons indicate that YAC operators utilizing an exponential fractional Rabotnov kernel outperform both RL and integer-time derivative operators in some aspects. For instance, the YAC operators utilizing an exponential fractional Rabotnov kernel exhibit superior accuracy and stability compared to the RL, CF, and AB, and integer-time derivative operators. Additionally, they are more efficient than the RL and integer-time derivative operators [55]. The YAC operators, which have an exponential fractional Rabotnov kernel, are easier to understand and don't have as many parts as the RL and integer time derivative operators. Consequently, they are more convenient to use and comprehend [56]. The exponential Ratputnov kernel is notable in the field of fractional calculus due to its capacity to expand the domain using exponential kernels that do not have singularities. It is widely used for modeling complex systems and dynamical systems, and it is valuable for deriving significant inequalities for stability analysis. Novel time and spatial fractional derivatives have utilized the exponential Ratputnov kernel, demonstrating its extensive versatility in diverse domains that incorporate fractional calculus.

The Ratputnov exponential kernel has shown effective in analyzing the fractional form of dynamical systems, such as the Lotka-Volterra model in mathematical biology. This use has facilitated a more profound comprehension of intricate dynamical behaviors. The exponential Ratputnov kernel, along with other fractional derivatives utilizing exponential kernels, can proficiently simulate intricate systems that demonstrate non-local effects, providing a more precise depiction of real-world events.

The introduction of fractional derivatives is anticipated to have a crucial impact on investigating the overall behavior of different materials, particularly in relation to partial exchanges such as thermoelasticity, fluidity, and other related phenomena. The incorporation of phase delays into the modified heat transfer equation employed for constructing the frame demonstrates that heat waves propagate in a natural manner and maintain a consistent magnitude. This discovery is significant because it showcases the capacity of the novel fractional derivatives to effectively simulate and forecast the behavior of thermoelastic materials under varying circumstances. The theory presented in

this study is very relevant to contemporary aerodynamic engineering challenges involving thermoplastic cylinders.

7.2. The influence of the speed of the heat flow

Thermal energy continuously transmits through a material in movable heat flows, which are part of the heat transfer processes under investigation. The analysis of these mobile heat transfers is essential in the study of heat conduction due to its wide-ranging applications in both technical and non-technological domains. Simulating and addressing the behavior of mobile heat fluxes is crucial for enhancing processes, guaranteeing even heat distribution, and controlling thermal effects on materials. This knowledge is extremely valuable for improving efficiency, quality, and reliability in a wide range of industrial and technological sectors. Heat can transfer in a mobile manner during various industrial operations such as heat treatment, metal forming, casting, smelting, welding, metal cutting, laser processing, metal plating, and plasma spraying. The interaction between heat flow and material qualities has a substantial impact on temperature variations, deformation, and thermal stresses in an elastic body.

This section attempts to evaluate and describe the impacts of mobile thermal flux fluxes on heat transfer, deformation, and thermal stresses using the Rabotnov fractional-exponential kernel (YAC) in the fractional thermoelasticity model. The goal is to forecast the behavior of the thermoelastic system being examined. This subsection specifically examines the impact of the velocity (υ) of a flowing heat flow on different fields. The remaining physical parameters, namely, $\tau_q = 0.2$, $\tau_\theta = 0.1$, $\omega = 15$, and $\alpha = 0.8$, are assumed to have a fixed value. Figures 7–11 display the changes in temperature, displacement, and stresses caused by varying velocities of the heat flux (υ) at speeds of 3, 5, and 8.

Figures 7–11 demonstrate a significant impact of the moving heat flux's velocity on the fluctuations of the studied field variables. When the heat transfer speed increases, there is a clear increase in displacement and thermal stresses [57]. This suggests that heat flows cause more significant deformation and stress on the elastic body. Moreover, it is evident that the heat flux intensity decreases exponentially with time, with a time constant of $1/\omega$. This suggests that the rate of heat transfer gradually diminishes with time.

Figure 7 clearly demonstrates the significant impact of heat transfer velocity (υ) on temperature changes (θ). As the body is elongated considerably in the direction of movement, the temperature profile θ surrounding the heat flow eventually reaches a state where it does not change with time, as shown in the diagram. The graph curves unambiguously demonstrate that an escalation in heat flow velocity υ results in a reduction in temperature magnitude θ. This discovery emphasizes the significant relationship between the speeds of heat flows in motion and changes in temperature, demonstrating a positive impact on temperature patterns. Typically, the duration to reach the maximum temperature θ is shorter than the time needed to attain a quasi-steady state. This phenomenon occurs when the initial rate of heat transfer from the flow to the substance surpasses its capacity to dissipate the heat. Consequently, the temperature of the material, denoted as θ, increases rapidly and reaches

its highest point before the heat flow condition can be characterized as quasi-steady, as stated in reference [58].

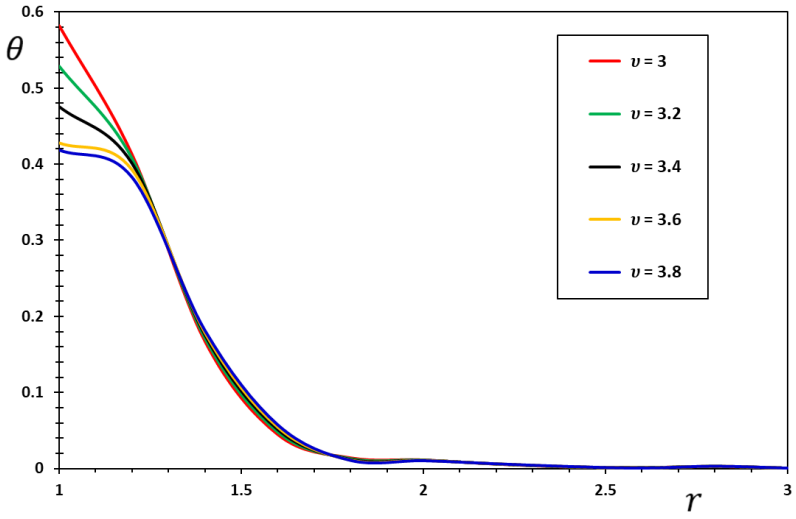

Figure 7. Temperature θ for different heat flow velocities υ.

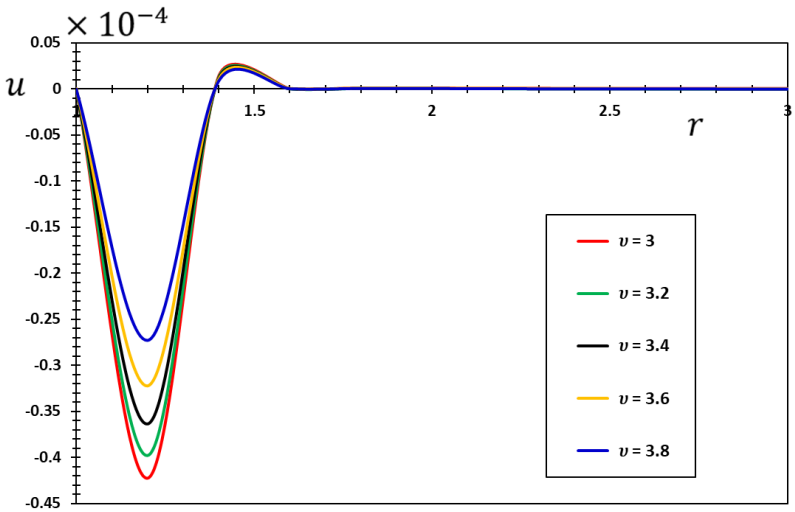

Figure 8. The displacement u for different heat flow velocities υ.

When the heat flow velocity increases, it delivers less energy per unit length, resulting in a narrower temperature range within the medium. Heat flowing at a higher speed spends less time in a particular region, leading to reduced heat transmission to the surrounding material, explaining this phenomenon. As a result, the temperature inside the material becomes more restricted, leading to a decrease in the maximum temperature and a reduction in the spatial range. Extensive research supporting this occurrence may be found in [58], which presents evidence that is consistent with the proposed explanation. The study demonstrates that when the rate of heat flow rises, the temperature distribution within the material becomes more limited, resulting in a lower maximum temperature and

a narrower geographical range. This discovery provides additional evidence for the accuracy of the model employed to elucidate the behavior of the system [59] since it corresponds with the anticipated behavior of a moving heat transfer.

Figure 8 illustrates the influence of heat flow velocity (υ) on the change in displacement (u). It is evident that an increase in heat flow velocity leads to a decrease in the displacement value. The decrease in thermal energy intensity per unit length at higher velocities explains this phenomenon. As a result, there is a lower temperature increase and, subsequently, a reduced displacement of the material [60]. The graph illustrates that the parameter υ has no major impact on the trajectory of the displacement pattern. Based on these results, we can conclude that the primary factor that determines the displacement of the material is the intensity of the heat source, not the speed of the source.

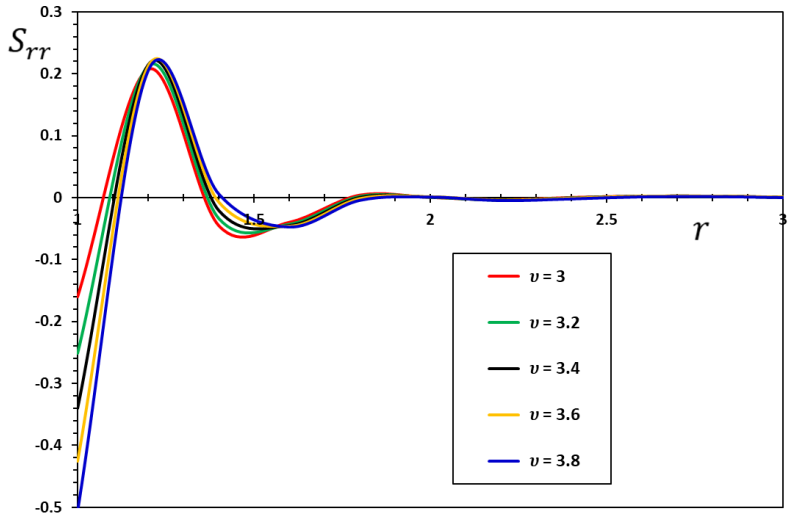

Figure 9. The stress S_{rr} for different heat flow velocities υ.

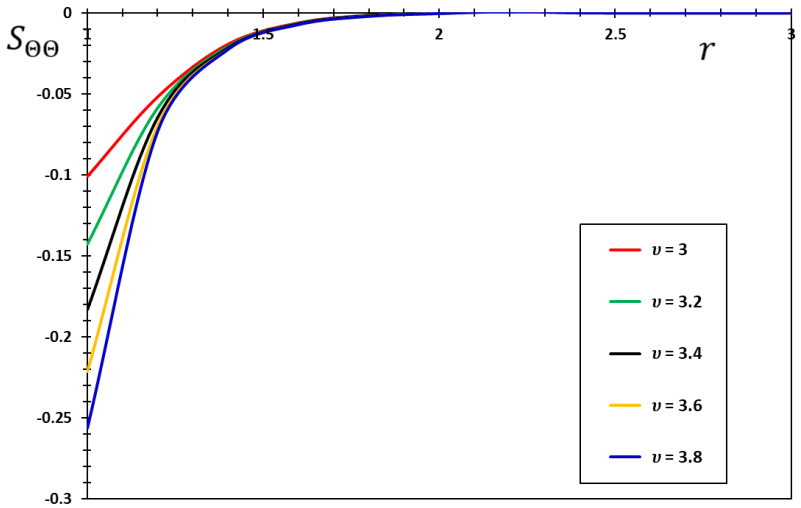

Figure 10. The stress $S_{\Theta\Theta}$ for different heat flow velocities υ.

Figures 9 and 10 illustrate the influence of the velocity parameter (υ) on the radial and annular pressures (S_{rr} and $S_{\Theta\Theta}$) in a material subjected to a heat source in motion. The stresses demonstrate a notable inclination to either escalate or diminish in magnitude based on the velocity parameter (υ) value. This pattern becomes apparent when the velocity parameter (υ) increases. As the velocity increases, the absolute pressures decline significantly. Consequently, the surrounding surfaces restrict the material, limiting its thermal expansion and deformation. This limitation causes the material to experience compressive thermal stresses, resulting in a decrease in the absolute pressures. Identifying the dynamics of radial and annular pressures in a material exposed to a mobile heat source is essential for a range of applications, such as heat treatment, metal forming, casting, and smelting, as well as the welding and cutting of certain metals. Examining the distribution of stress allows for process optimization, improves product quality, and ensures safe and efficient functioning in a variety of industrial developments.

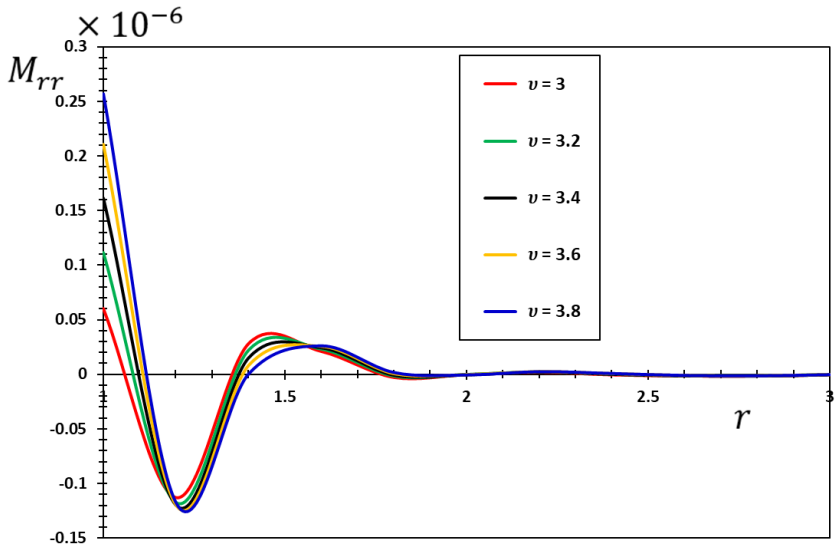

Figure 11. The Maxwell's stress M_{rr} for different heat flow velocities υ.

Figure 11 illustrates the correlation between Maxwell stress (M_{rr}) and the velocity coefficient (υ). The image demonstrates that the velocity parameter (υ) has a negligible influence on Maxwell's stress (M_{rr}), similar to its impact on displacement (u). A plausible explanation for this phenomenon is that the heat flux being applied is traveling at a consistent velocity (υ), and the distance covered by the heat source can be calculated using the equation $r = \upsilon t$, which takes into consideration the amount of time that has passed since instant t. Therefore, the temperature increase can be attributed to a rise in the amount of heat emitted from the source when $r = \upsilon t$. These findings indicate that the fundamental determinant of the Maxwell stress within the system is the intensity of the heat source rather than its speed. During extended simulations, it is possible to build a nearly constant temperature field, and this field remains unchanged in the coordinate system that moves along with the heat source. This discovery is consistent with the findings reported in reference [61], which also suggest the presence of

a nearly constant temperature distribution in a material that is heated by a heat source in motion.

The temperature distribution in a material subjected to a moving heat flow is affected by various elements, such as the material's qualities, heat source characteristics, and boundary conditions. Addressing the dynamics of temperature distribution in these situations is crucial for a range of practical uses, such as heat treatment, metal forming, casting, smelting, welding, and the cutting of certain metals. Through the analysis and understanding of temperature distribution, it is possible to improve industrial processes, enhance product quality, and guarantee safe and efficient operations.

8. Conclusions

Utilizing a two-phase delay fractional thermoelasticity model enables a more accurate depiction of the thermomechanical elastic interactions in materials. This work presents a novel thermoelastic model for thermal conductivity that integrates local fractional differential operators and non-anomalous kernels. The paper presents a novel fractional derivative operator that utilizes a non-singular kernel. This operator is based on the fractional exponential Rabotnov function, which was presented by YAC. The model was utilized to analyze the thermoelastic and mechanical responses of an infinite medium with a spherical cavity under the influence of a moving thermal flow. The model is regarded as adaptable and suitable to thermoelastic materials with intricate geometries and diverse boundary conditions, which are pertinent to fields such as geophysics, aerospace engineering, nuclear engineering, and biomedical engineering. This research enhances the comprehension of thermomechanical responses in materials and offers a helpful analytical tool for studying many practical scenarios by integrating the two-phase delay fractional thermoelasticity model and the innovative fractional derivative operator. The studies and discussions have resulted in some noteworthy conclusions:

• The use of fractional differential operators in the heat conduction equation allows for a more precise comprehension of how a material responds to heat, taking into account aspects such as the duration of phase delays and the dynamic heat flow.

• The order of fractional differentiation and the use of fractional differential operators significantly affect several physical domains, such as temperature distribution and thermal stresses.

• In elastic media, the order of fractional derivatives is critical to reducing mechanical and thermal waves. Hence, the fractional order coefficient can be used as a new parameter to assess the heat transport and conductivity capacity of elastic materials, akin to thermal conductivity coefficients and other physical factors. Additionally, it offers valuable information on enhancing the effectiveness of thermoplastic materials.

• In an elastic medium, a heat wave propagates at a measurable velocity that corresponds to empirical data. This suggests that the proposed fractional heat conduction model deviates greatly from the usual Fourier equation, which anticipates unlimited wave diffusion.

• When used in thermoelastic simulations, the YAC fractional operator demonstrates its superiority over conventional fractional operators. It can be efficiently utilized to address interconnected physical issues, such as biothermia and viscoelasticity.

• As the velocity of the heat flow rises, the temperature pattern in the material becomes more

restricted, with lower maximum temperature values and a smaller spatial range. This can be attributed to the heightened restriction on the temperature distribution of the material. At greater speeds, the amount of thermal energy per unit length reduces, leading to reduced temperature increases and smaller movements of the material.

• The study findings have practical implications for optimizing industrial operations, promoting product quality, and ensuring process safety and efficiency, particularly in situations involving heat transfer and exposure to intricate thermal and mechanical pressures.

Author contributions

Ahmed Abouelregal: Writing-original draft, writing-review and editing; Faisal Alsharif: Funding acquisition, writing-review and editing, supervision; Hashem Althagafi: Writing-review and editing, supervision; Yazeed Alhassan: Methodology, writing-review and editing, supervision. All authors have read and approved the final version of the manuscript for publication.

Conflict of interest

The authors have not disclosed any conflict of interest regarding this work's research, writing, and publication.

Funding

This work was funded by the Deanship of Scientific Research at Jouf University through the Fast-track Research Funding Program.

References

1. A. A. Kilbas, H. M. Srivastava, J. J. Trujillo, *Theory and applications of fractional differential equations*, Elsevier, 2006.
2. I. Podlubny, *Fractional differential equations: An introduction to fractional derivatives, fractional differential equations, to methods of their solution and some of their applications*, Elsevier, 1998.
3. X. J. Yang, *General fractional derivatives: Theory, methods and applications*, CRC Press, 2019.
4. A. Atangana, D. Baleanu, New fractional derivatives with nonlocal and non-singular kernel: Theory and application to heat transfer model, *Therm. Sci.*, **20** (2016), 763–769. https://doi.org/10.2298/TSCI16011108A
5. M. Caputo, M. Fabrizio, A new definition of fractional derivative without singular kernel, *Prog. Frac. Diff. Appl.*, **1** (2015), 73–85. http://dx.doi.org/10.12785/pfda/010201
6. X. J. Yang, M. Abdel-Aty, C. Cattani, A new general fractional-order derivative with Rabotnov fractional-exponential kernel applied to model the anomalous heat transfer, *Therm. Sci.*, **23** (2019), 1677–1681. https://doi.org/10.2298/TSCI180320239Y
7. R. Khalil, M. Al Horani, A. Yousef, M. Sababheh, A new definition of fractional derivative, *J. Comput. Appl. Math.*, **264** (2014), 65–70. https://doi.org/10.1016/j.cam.2014.01.002
8. V. V. Uchaikin, *Fractional derivatives for physicists and engineers*, Berlin: Springer, 2013.

9. X. J. Yang, F. Gao, Y. Ju, *General fractional derivatives with applications in viscoelasticity*, Academic Press, 2020.
10. K. A. Abro, A. Atangana, A comparative study of convective fluid motion in rotating cavity via Atangana-Baleanu and Caputo-Fabrizio fractal-fractional differentiations, *Europ. Phys. J. Plus*, **135** (2020), 1–16. https://doi.org/10.1140/epjp/s13360-020-00136-x
11. A. A. Shaikh, S. Qureshi, Comparative analysis of Riemann-Liouville, Caputo-Fabrizio, and Atangana-Baleanu integrals, *J. Appl. Math. Comput. Mech.*, **21** (2022), 91–101. https://doi.org/10.17512/jamcm.2022.1.08
12. M. M. AlBaidani, F. Aljuaydi, N. S. Alharthi, A. Khan, A. H. Ganie, Study of fractional forced KdV equation with Caputo-Fabrizio and Atangana-Baleanu–Caputo differential operators, *AIP Adv.*, **14** (2024), 015340. https://doi.org/10.1063/5.0185670
13. B. K. Jha, I. O. Oyelade, P. B Malgwi, The Caputo-Fabrizio (CF) and Atangana-Baleanu in Caputo sense (ABC) fractional time-derivative approach on transient free convection flow between two vertical parallel plates: A semi-analytical solution, *Heat Trans.*, **51** (2022), 841–865. https://doi.org/10.1002/htj.22332
14. S. A. Gulalai, F. A. Rihan, S. Ahmad, F. A. Rihan, A. Ullah, Q. M. Al-Mdallal, et al., Nonlinear analysis of a nonlinear modified KdV equation under Atangana Baleanu Caputo derivative, *AIMS Mathematics*, **7** (2022), 7847–7865. https://doi.org/10.3934/math.2022439
15. M. M. Khader, J. E. Macías-Díaz, A. Román-Loera, K. M. Saad, A note on a fractional extension of the Lotka-Volterra model using the Rabotnov exponential kernel, *Axioms*, **13** (2024), 71. https://doi.org/10.3390/axioms13010071
16. M. M. Khader, J. E. Macías-Díaz, K. M. Saad, W. M. Hamanah, Vieta-Lucas polynomials for the Brusselator system with the Rabotnov fractional-exponential kernel fractional derivative, *Symmetry*, **15** (2023), 1619. https://doi.org/10.3390/sym15091619
17. A. F. Aboubakr, G. M. Ismail, M. M. Khader, M. A. Abdelrahman, A. M. AbdEl-Bar, M. Adel, Derivation of an approximate formula of the Rabotnov fractional-exponential kernel fractional derivative and applied for numerically solving the blood ethanol concentration system, *AIMS Mathematics*, **8** (2023), 30704–30716. https://doi.org/10.3934/math.20231569
18. S. Kumar, B. Ahmad, A new numerical study of space-time fractional advection-reaction-diffusion equation with Rabotnov fractional-exponential kernel, *Num. Meth. Part. Diff. Equ.*, **38** (2022), 457–469. https://doi.org/10.1002/num.22647
19. H. Parkus, *Thermoelasticity*, Springer, 2012.
20. W. Nowacki, *Dynamic problems of thermoelasticity*, Springer, 1975.
21. M. A. Biot, Thermoelasticity and irreversible thermodynamics, *J. Appl. Phys.*, **27** (1956), 240–253. https://doi.org/10.1063/1.1722351
22. J. L. Nowinski, *Theory of thermoelasticity with applications* (Vol. 3), Alphen aan den Rijn: Sijthoff & Noordhoff International Publishers, 1978.
23. V. D. Kupradze, *Three-dimensional problems of elasticity and thermoelasticity*, Elsevier, 2012.
24. J. Ignaczak, M. Ostoja-Starzewski, *Thermoelasticity with finite wave speeds*, OUP Oxford, 2009.
25. H. Lord, Y. Shulman, A generalized dynamical theory of thermoelasticity, *J. Mech. Phys. Solids*, **15** (1967), 299–309. https://doi.org/10.1016/0022-5096(67)90024-5
26. A. E. Green, K. A. Lindsay, Thermoelasticity, *J. Elas.*, **2** (1972), 1–7. http://dx.doi.org/10.1007/BF00045689

27. A. E. Green, P. M. Naghdi, Thermoelasticity without energy dissipation, *J. Elas.*, **31** (1993), 189–208. http://dx.doi.org/10.1007/BF00044969
28. A. E. Green, P. M. Naghdi, On undamped heat waves in an elastic solid, *J. Therm. Stress.*, **15** (1992), 253–264. https://doi.org/10.1080/01495739208946136
29. D. Y. Tzou, Experimental support for the lagging behavior in heat propagation, *J. Therm. Heat Trans.*, **9** (1995), 686–693. https://doi.org/10.2514/3.725
30. D. Y. Tzou, *Macro-to microscale heat transfer: The Lagging behavior*, Washington, DC: Taylor and Francis, 1996.
31. D. Y. Tzou, A unified field approach for heat conduction from macro-to micro-scales, *ASME J. Heat Mass Tran.*, **117** (1995), 8–16. https://doi.org/10.1115/1.2822329
32. C. Li, F. Zeng, *Numerical methods for fractional calculus* (Vol. 24), CRC Press, 2015.
33. A. Atangana, D. Baleanu, Caputo-Fabrizio derivative applied to groundwater flow within confined aquifer, *J. Eng. Mech.*, **143** (2017), D4016005. https://doi.org/10.1061/(ASCE)EM.1943-7889.0001091
34. X. X Yu, Y. Zhang, H. Sun, C. Zheng, Time fractional derivative model with Mittag-Leffler function kernel for describing anomalous diffusion: Analytical solution in bounded-domain and model comparison, *Chaos Soliton Fract.*, **115** (2018), 306–312. https://doi.org/10.1016/j.chaos.2018.08.026
35. Y. Rabotnov, Equilibrium of an elastic medium with after-effect, *Fract. Calc. Appl. Anal.*, **17** (2014), 684–696. https://doi.org/10.2478/s13540-014-0193-1
36. D. Khan, P. Kumam, W. Watthayu, K. Sitthithakerngkiet, M. Y. Almusawa, Application of new general fractional-order derivative with Rabotnov fractional–exponential kernel to viscous fluid in a porous medium with magnetic field, *Math. Meth. Appl. Sci.*, **46** (2023), 13457–13468. https://doi.org/10.1002/mma.9264
37. H. Parkus, *Magneto-thermoelasticity* (Vol. 118), Vienna-New York: Springer-verlag, 1972.
38. M. A. Ezzat, A. S. El-Karamany, A. A. El-Bary, Magneto-thermoelasticity with two fractional order heat transfer, *J. Assoc. Arab Univ. Basic Appl. Sci.*, **19** (2016), 70–79. https://doi.org/10.1016/j.jaubas.2014.06.009
39. G. Paria, Magneto-elasticity and magneto-thermo-elasticity, *Adv. Appl. Mech.*, **10** (1966), 73–112. https://doi.org/10.1016/S0065-2156(08)70394-6
40. X. Wang, J. S. Lee, X. Zheng, Magneto-thermo-elastic instability of ferromagnetic plates in thermal and magnetic fields, *Int. J. Solids Struct.*, **40** (2003), 6125–6142. https://doi.org/10.1016/S0020-7683(03)00297-X
41. A. E. Abouelregal, R. Alanazi, H. M. Sedighi, Thermal plane waves in unbounded non-local medium exposed to a moving heat source with a non-singular kernel and higher order time derivatives, *Eng. Anal. Bound. Elem.*, **140** (2022), 464–475. https://doi.org/10.1016/j.enganabound.2022.04.032
42. A. M. Cohen, *Numerical methods for Laplace transform inversion* (Vol. 5), Springer, 2007.
43. O. Taiwo, J. Schultz, V. Krebs, A comparison of two methods for the numerical inversion of Laplace transforms, *Comput. Chem. Eng.*, **19** (1995), 303–308. https://doi.org/10.1016/0098-1354(94)00055-S
44. G. Honig, U. Hirdes, A method for the numerical inversion of Laplace transforms, *J. Comput. Appl. Math.*, **10** (1984), 113–132. https://doi.org/10.1016/0377-0427(84)90075-X

45. A. Soleiman, A. E. Abouelregal, K. M. Khalil, M. E. Nasr, Generalized thermoviscoelastic novel model with different fractional derivatives and multi-phase-lags, *Eur. Phys. J. Plus*, **135** (2020), 851. https://doi.org/10.1140/epjp/s13360-020-00842-6
46. A. E. Abouelregal, M. Alesemi, Vibrational analysis of viscous thin beams stressed by laser mechanical load using a heat transfer model with a fractional Atangana-Baleanu operator, *Case Stud. Therm. Eng.*, **34** (2022), 102028. https://doi.org/10.1016/j.csite.2022.102028
47. A. U. Rehman, F. Jarad, M. B. Riaz, A fractional study of MHD Casson fluid motion with thermal radiative flux and heat injection/suction mechanism under ramped wall condition: Application of Rabotnov exponential kernel, *Acta Mech. Autom.*, **18** (2024), 84–92. https://doi.org/10.2478/ama-2024-0011
48. Y. Z. Povstenko, Fractional heat conduction equation and associated thermal stress, *J. Therm. Stress.*, **28** (2004), 83–102. https://doi.org/10.1080/014957390523741
49. A. U. Rehman, M. B. Riaz, A. Atangana, Time fractional analysis of Casson fluid with Rabotnov exponential memory based on the generalized Fourier and Fick's law, *Sci. Afr.*, **17** (2022), e01385. https://doi.org/10.1016/j.sciaf.2022.e01385
50. M. Yavuz, N.Sene, Fundamental calculus of the fractional derivative defined with Rabotnov exponential kernel and application to nonlinear dispersive wave model, *J. Ocean Eng. Sci.*, **6** (2021), 196–205. https://doi.org/10.1016/j.joes.2020.10.004
51. D. Mortari, Representation of fractional operators using the theory of functional connections, *Mathematics*, **11** (2023), 4772. https://doi.org/10.3390/math11234772
52. X. J. Yang, M. Ragulskis, T. Tana, A new general fractional-order derivative with Rabotnov fractional-exponential kernel, *Therm. Sci.*, **23** (2019), 3711–3718. https://doi.org/10.2298/TSCI180825254Y
53. S. Kumar, S. Ghosh, B. Samet, E. F. D. Goufo, An analysis for heat equations arises in diffusion process using new Yang-Abdel-Aty-Cattani fractional operator, *Math. Meth. Appl. Sci.*, **43** (2020), 6062–6080. https://doi.org/10.1002/mma.6347
54. Q. Khan, A. Suen, H. Khan, P. Kumam, Comparative analysis of fractional dynamical systems with various operators, *AIMS Mathematics*, **8** (2023), 13943–13983. https://doi.org/10.3934/math.2023714
55. M. M. Khader, J. E. Macías-Díaz, A. Román-Loera, K. M. Saad, A note on a fractional extension of the Lotka–Volterra model using the Rabotnov exponential kernel, *Axioms*, **13** (2024), 71. https://doi.org/10.3390/axioms13010071
56. I. V. Malyk, M. Gorbatenko, A. Chaudhary, S. Sharma, R. S. Dubey, Numerical solution of nonlinear fractional diffusion equation in framework of the Yang-Abdel-Cattani derivative operator, *Fractal Fract.*, **5** (2021), 64. https://doi.org/10.3390/fractalfract5030064
57. H. Belghazi, M. El Ganaoui, J. C. Labbe, Analytical solution of unsteady heat conduction in a two-layered material in imperfect contact subjected to a moving heat source, *Int. J. Therm. Sci.*, **49** (2010), 311–318. https://doi.org/10.1016/j.ijthermalsci.2009.06.006
58. J. Ma, Y. Sun, B. Li, Spectral collocation method for transient thermal analysis of coupled conductive, convective and radiative heat transfer in the moving plate with temperature dependent properties and heat generation, *Int. J. Heat Mass Trans.*, **114** (2017), 469–482. https://doi.org/10.1016/j.ijheatmasstransfer.2017.06.082

59. A. E. Abouelregal, M. Marin, S. M. Abusalim, An investigation into thermal vibrations caused by a moving heat supply on a spinning functionally graded isotropic piezoelectric bounded rod, *Mathematics*, **11** (2023), 1739. https://doi.org/10.3390/math11071739
60. A. E. Abouelregal, Generalized thermoelasticity for an isotropic solid sphere indual-phase-lag of heat transfer with surface heat flux, *Int. J. Comput. Meth. Eng. Sci. Mech.*, **12** (2011), 96–105. https://doi.org/10.1080/15502287.2010.548172
61. A. E. Abouelregal, Rotating magneto-thermoelastic rod with finite length due to moving heat sources via Eringen's nonlocal model, *J. Comput. Appl. Mech.*, **50** (2019), 118–126. https://doi.org/10.22059/jcamech.2019.275893.360